

Contents lists available at [SciVerse ScienceDirect](http://SciVerse.Sciencedirect.com)

Radiation Measurements

journal homepage: www.elsevier.com/locate/radmeas

Calibration of PADC-based neutron area dosimeters in the neutron field produced in the treatment room of a medical LINAC

R. Bedogni^{a,*}, C. Domingo^b, A. Esposito^a, A. Gentile^a, M.J. García-Fusté^b, M. de-San-Pedro^b, L. Tana^c, F. d'Errico^d, R. Ciolini^d, A. Di Fulvio^d^a INFN – LNF Istituto Nazionale di Fisica Nucleare, Laboratori Nazionali di Frascati, Via E. Fermi n. 40 00044 Frascati, Roma, Italy^b Grup de Recerca en Radiacions Ionizants, Departament de Física, Universitat Autònoma de Barcelona, E-08193 Bellaterra, Spain^c A.O. Universitaria Pisana, Ospedale S. Chiara, Via Bonanno Pisano, Pisa, Italy^d Dipartimento di Ingegneria Meccanica, Nucleare e della Produzione (DIMNP), Università di Pisa, Largo Lazzarino 1, I-56100 Pisa

ARTICLE INFO

Article history:

Received 15 December 2011

Accepted 13 April 2012

Keywords:

Neutron dosimetry
Neutron spectrometry
PADC
CR-39
Bonner spheres
Dysprosium
Activation foils
FRUIT unfolding code
Medical LINAC

ABSTRACT

PADC-based nuclear track detectors have been widely used as convenient ambient dosimeters in many working places. However, due to the large energy dependence of their response in terms of ambient dose equivalent ($H^*(10)$) and to the diversity of workplace fields in terms of energy distribution, the appropriate calibration of these dosimeters is a delicate task. These are among the reasons why ISO has introduced the 12789 Series of Standards, where the *simulated workplace neutron fields* are introduced and their use to calibrate neutron dosimeters is recommended. This approach was applied in the present work to the UAB PADC-based nuclear track detectors. As a suitable workplace, the treatment room of a 15 MV Varian CLINAC DHX medical accelerator, located in the Ospedale S. Chiara (Pisa), was chosen. Here the neutron spectra in two points of tests (1.5 m and 2 m from the isocenter) were determined with the INFN-LNF Bonner Sphere Spectrometer equipped with Dysprosium activation foils (Dy-BSS), and the values of $H^*(10)$ were derived on this basis. The PADC dosimeters were exposed in these points. Their workplace specific $H^*(10)$ responses were determined and compared with those previously obtained in different simulated workplace or reference (ISO 8529) neutron fields.

© 2012 Elsevier Ltd. All rights reserved.

1. Introduction

Medical electron accelerators above 10 MeV constitute an important category of workplaces where accurate neutron dosimetry measurements are requested for two main purposes: (1) the occupational radiation protection and (2) the patient protection. The importance of the latter has significantly increased in recent years, since it is a consolidated opinion in the medical physics community that the neutron irradiation of peripheral organs during radiotherapy sessions is significantly related to the occurrence of secondary cancers (Followill et al., 2007; Hall and Wu, 2003; Hall and Phil, 2006). PADC-based nuclear track detectors are used as suitable ambient dosimeters in these fields, mainly due to their photon-insensitivity (Domingo et al., 2009). However, due to the large energy dependence of their response in terms of ambient dose equivalent ($H^*(10)$), their use should be preceded by a careful selection of the calibration factor. The approach

recommended in the ISO 12789 Series of Standards (ISO, 2008a; ISO, 2008b) is applied in this study. The PADC-based nuclear track detectors from UAB were used. The treatment room of the 15 MV Varian CLINAC DHX medical accelerator located in the Ospedale S. Chiara (Pisa), was chosen to act as *simulated workplace neutron field*. Here the neutron spectra in two points of tests (point A, located at 1.5 m from the isocenter, and point B, at 2 m from the isocenter) were determined with the INFN-LNF Bonner Sphere Spectrometer equipped with Dysprosium activation foils (called Dy-BSS) [Bedogni et al., 2010] and the reference values of $H^*(10)$ were derived on this basis. The PADC dosimeters were exposed in these points. Their workplace specific $H^*(10)$ responses were determined and compared with those previously obtained in simulated workplace fields available at PTB (Kluge et al., 1996; ISO 2008a) (total ^{252}Cf field or ^{252}Cf field behind shadowing object) or a reference $^{241}\text{Am-Be}$ field.

2. The simulated workplace field and its characterization

The treatment room of the 15 MV Varian CLINAC DHX medical accelerator and the locations of the points of test are shown in

* Corresponding author. Tel.: +39 (0) 694032608; fax: +39 (0)694032364.
E-mail address: roberto.bedogni@lnf.infn.it (R. Bedogni).

Fig. 1. The characteristics of Dy-BSS depend on the combination of the large thermal neutron cross-section of Dy (2700 b at 0.025 eV) and the short half live of the activation products (2.334 h): (1) Sensitivity for operational measurements: the specific activity obtained after irradiation of few minutes, representative of the short times allowed for dosimetry sessions in most operational conditions (e.g. medical LINACs) is significantly higher than for the commonly used gold foils-based BSS (Thomas et al., 2002); (2) Capability to provide rapid results: the foils are counted in situ with a portable beta counter; (3) Disadvantage: if all spheres are exposed at the same time and only one counter is available, the short half live of the activation products would constitute a limitation in the counting procedure. This system has been used already to characterize neutron fields from photo-neutron (Bedogni et al., 2011) or high-energy spallation sources (Bedogni et al., 2009, 2010a). The polyethylene spheres used in this work are: 2 in., 2.5 in., 3 in., 3.5 in., 4 in., 4.5 in., 5 in., 7 in., 8 in., 10 in. and 12 in. (Spheres are usually identified with their diameter expressed in inches). In every exposure, a natural Dysprosium foil with diameter 12 mm, thickness 0.1 mm, and purity >99.9% is positioned in the sphere centre through a specially designed aluminium-polyethylene cylindrical holder. Thermal and epithermal neutrons activate the ^{164}Dy isotope (28.2% abundance in natural Dysprosium) producing ^{165}Dy , a beta-gamma emitter with half-life 2.334 h. The main beta emission (83%) has end-point energy 1.287 MeV, whilst all significant photon emissions have energies lower than 53 keV. The foils are counted using a commercial beta counter.

The response matrix of the Dy-BSS was calculated with MCNPX (Waters, 2002) and verified in the continuous spectrum from a ^{252}Cf source (Bedogni et al., 2010), ranging from 10 keV to 15 MeV, as well as in a 2.5 MeV quasi mono-chromatic beam (Bedogni et al., 2011a). These experiments indicated that the overall uncertainty of the response matrix might be reasonably estimated as $\sim \pm 2.5\%$.

The Dy-BSS response matrix is expressed in terms of saturation specific activity (or saturation count rate in the beta counter) per unit neutron fluence rate. The procedure needed to obtain this quantity from the result of the beta counting implies corrections for the detector efficiency, the decay between the end of the irradiation and the beginning of the measurement, the decay during the measurement and the fraction of the saturation activity reached during the irradiation.

For the measurement campaign described in this work the accelerator output was tuned to 500 MU min^{-1} and the treatment field was $10 \text{ cm} \times 10 \text{ cm}$ at the isocenter. The Dy-BSS was sequentially exposed in point A and point B. Each sphere was exposed to 1500 MU. After irradiation the foils were counted for the

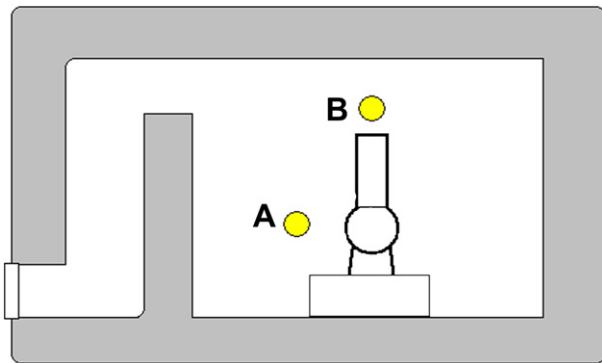


Fig. 1. The 15 MV Varian CLINAC DHX medical accelerator of the Ospedale S. Chiara (Pisa) and the locations of the points of test. Dimensions of the room are approx. $8 \text{ m} \times 6.7 \text{ m} \times 3 \text{ m}$ (height).

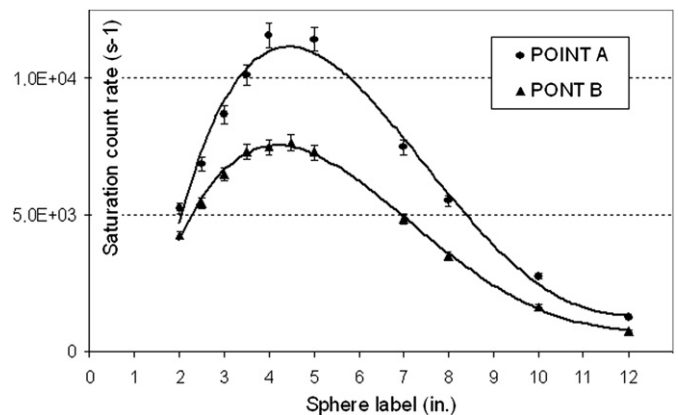


Fig. 2. Readings of the Dy-BSS exposed in points A and B as a function of the sphere diameter. Continuous curves represent polynomial interpolations (4th degree).

time required to achieve a counting uncertainty of $\pm 1\%$ (one s.d.). Counting time ranged from 2 to 4 min. The reproducibility of the counter is routinely checked using a calibration source. Additional tests were performed by inserting, counting and extracting the same foil a number of times. These tests allowed calculating an additional $\pm 2\%$ reading uncertainty.

The consistency of the sets of measurements was verified through the curves of Fig. 2, representing the Dy-BSS readings as a function of the sphere diameter. As explained by Alevra and Thomas (2003), these curves should be smooth if the measurements are performed under “...stable conditions, using the right monitors, and are not affected by supplementary uncertainties of unexplained origin”.

After the consistency check, the Dy-BSS readings were unfolded using the FRUIT code (Bedogni et al., 2007). An evaporative model was adopted to parameterize the fast neutron component.

The unfolded neutron spectra are shown in Fig. 3. The best estimation of the fluence rate (in $\text{cm}^{-2} \text{ s}^{-1}$), the neutron fluence per monitor unit (in $\text{cm}^{-2} \text{ MU}^{-1}$) and the ambient dose equivalent per unit absorbed dose to water at the isocenter (in mSv Gy^{-1}) are given in Table 1.

The unfolding code provides uncertainties for all numerical results: the fluence, the ambient dose equivalent, the parameters describing the neutron spectrum, the fractions of fluence under

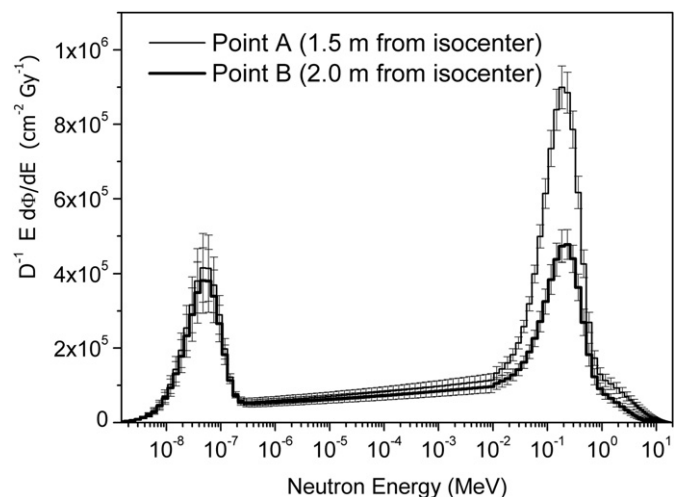


Fig. 3. Unfolded neutron spectra for points A and B, in equi-lethargy representation and normalized to the unit absorbed dose to water in the isocenter.

Table 1
Spectrum-integrated quantities for points A and B in the LINAC treatment room.

Quantity	Point A	Point B
$d\phi/dt$ ($\text{cm}^{-2} \text{s}^{-1}$)	$(3.18 \pm 0.10) \cdot 10^5$	$(2.28 \pm 0.09) \cdot 10^5$
ϕ/D ($\text{cm}^{-2} \text{MU}^{-1}$)	$(3.82 \pm 0.14) \cdot 10^4$	$(2.74 \pm 0.11) \cdot 10^4$
$H^*(10)/D$ (mSv Gy^{-1})	0.383 ± 0.018	0.224 ± 0.013

given energy intervals, and the numerical spectrum specified by per-bin. These come from the propagation of the uncertainties of the input data (combined uncertainties of the Dy-BSS reading and of the response matrix) through the unfolding procedure. This propagation is done by randomly generating a large number of sets of BSS counts, using the input uncertainties as amplitude of the Gaussian perturbation, then separately unfolding each set. The statistical distributions of the results are used to derive the uncertainties reported in Table 1 and in Fig. 3.

The coherence between the unfolded spectra and the experimental data can be demonstrated by folding the Dy-BSS response matrix with the unfolded spectra, and comparing the resulting “simulated” counts with the experimental counts. This calculation was done for points A and B, and the maximum difference was 4%. This figure is coherent with the uncertainties associated to the input data: $\sim 2\%$ for the Dy-BSS readings and $\sim 2.5\%$ for the Dy-BSS response matrix.

3. PADC dosimeters calibration

The PADC-based planar neutron dosimeter of UAB (Garcia et al., 2005) is a stack formed by: (1) a 3 mm polyethylene n-p radiator, (2) 0.3 mm of Makrofol-ED polycarbonate (manufactured by Bayer AG) foil, with the purpose of flattening the energy dependence of the response, (3) 0.1 mm of Nylon acting as thermal neutron to proton converter through the $^{14}\text{N}(n, p)^{14}\text{C}$ reaction, (4) 0.5 mm of PADC to register the tracks, and (5) a 5 mm thick methacrylate holder. The PADC elements are processed in a 3 step Electro-Chemical Etching (ECE). This configuration was originally studied to yield a reasonably flat energy dependence of the personal dose equivalent response. Limited to the energy domain 0.3–16 MeV, the response in terms of ambient dose equivalent was studied (Domingo et al., in this issue). The $H^*(10)$ response in the epithermal domains is expected to be very poor, because no back-scattered neutrons are present when irradiating in free-in-air conditions. On the contrary, the backscattered neutrons are

Table 2
Results of the exposure of PADC dosimeters in points A and B in the LINAC treatment room. The corresponding values of $H^*(10)$ are also reported.

	Point A	Point B
Net track density (cm^{-2})	$(7.6 \pm 1.2) \cdot 10^3$	$(1.22 \pm 0.15) \cdot 10^3$
Reference $H^*(10)$ (mSv)	23.0 ± 1.1	3.5 ± 0.2

Table 3
 $H^*(10)$ response of UAB PADC dosimeters derived “in field” (Points A and B), in a $^{241}\text{Am-Be}$ reference field and in the PTB simulated workplaces (total ^{252}Cf field and shadowed ^{252}Cf field). Uncertainties are due, in practice, to the counting statistics only.

	$H^*(10)$ response ($\text{cm}^{-2} \text{mSv}^{-1}$)
Point A (in field)	330 ± 50
Point B (in field)	350 ± 50
$^{241}\text{Am-Be}$	370 ± 40
Total ^{252}Cf field	350 ± 20
^{252}Cf field shadowing object	115 ± 11

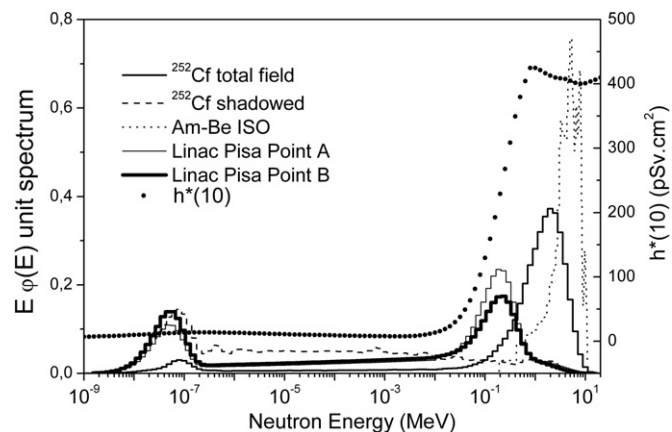


Fig. 4. Spectra of the calibration fields used in this work compared with the energy-dependent fluence-to-ambient dose equivalent conversion factor, $h^*(10)$.

responsible for almost the totality of the epithermal $H_p(10)$ response, determined in presence of phantom.

Two sets of three UAB dosimeters were exposed free-in-air in points A and B to the neutron field corresponding to 6000 and 1550 MU, respectively. The orientation of their surfaces was normal to the line joining the LINAC target to the point of test.

The net track density (total minus background) and the corresponding reference $H^*(10)$ values, obtained from the spectrometry, are reported in Table 2. The corresponding workplace specific $H^*(10)$ responses, derived “in field” according to the ISO 12789 approach, are reported in Table 3. The same Table reports also the $H^*(10)$ responses previously obtained in a reference $^{241}\text{Am-Be}$ field and two simulated workplace fields available at PTB (Kluge et al., 1996; ISO, 2008a) (total ^{252}Cf field and ^{252}Cf field behind a shadowing object). The spectra of these fields are shown, together with the energy-dependent fluence-to- $H^*(10)$ conversion factor, in Fig. 4. From Table 3 it is evident that all $H^*(10)$ responses are compatible, except that obtained in the shadowed ^{252}Cf field. In other words, the calibrations performed in the $^{241}\text{Am-Be}$, in the total ^{252}Cf field, or directly in points A and B are all equivalent for the purposes of determining the ambient dose equivalent in the LINAC treatment room.

Compared with the other fields, the “shadowed Cf” is significantly softer (See Fig. 4). This, together with poor dosimeter response in the low-energy domain, explain the difference observed in the $H^*(10)$ responses.

4. Conclusions

The neutron fields in two points of the treatment room of a 15 MV medical LINAC have been characterized using a recently developed Bonner Sphere Spectrometer based on Dysprosium activation foils. Following the suggestion of ISO 12789 Series of Standards, these fields have been considered as simulated workplace neutron fields and used to calibrate PADC-based neutron dosimeters. The related $H^*(10)$ responses have been compared with those previously obtained in simulated workplace fields available at PTB (total ^{252}Cf field or ^{252}Cf field behind shadowing object) or a reference $^{241}\text{Am-Be}$ field. The $H^*(10)$ responses derived in the $^{241}\text{Am-Be}$ and in the total ^{252}Cf field are equivalent to those directly measured in the LINAC room (points A and B). These are all very different from that obtained in the softer shadowed Cf field. The difference may be explained relying on the energy composition of the fields and on the energy-dependent response of the PADC dosimeters.

References

- Alevra, A.V., Thomas, D.J., 2003. Neutron spectrometry in mixed fields: multisphere spectrometers. *Radiat. Prot. Dosimetry* 107 (1–3), 37–72.
- Bedogni, R., Domingo, C., Esposito, A., Fernández, F., 2007. FRUIT: an operational tool for multisphere neutron spectrometry in workplaces. *Nucl. Instr. Meth. A* 580, 1301–1309.
- Bedogni, R., Esposito, A., Andreani, C., Senesi, R., De Pascale, M.P., Picozza, P., Pietropaolo, A., Gorini, G., Frost, C.D., Ansell, S., 2009. Characterization of the neutron field at the ISIS-VESUVIO facility by means of a Bonner sphere spectrometer. *Nucl. Instr. Meth. A* 612, 143–148.
- Bedogni, R., Ferrari, P., Gualdrini, G., Esposito, A., 2010. Design and experimental validation of a Bonner sphere spectrometer based on dysprosium activation foils. *Radiat. Meas.* 45, 1201–1204.
- Bedogni, R., Esposito, A., Gomez-Ros, J.M., 2010a. Response matrix of an extended range Bonner sphere spectrometer for the characterization of collimated neutron beams. *Radiat. Meas.* 45, 1205–1212.
- Bedogni, R., Quintieri, L., Buonomo, B., Esposito, A., Mazzitelli, G., Foggetta, L., Gómez-Ros, J.M., 2011. Experimental and numerical characterization of the neutron field produced in the n@BTF Frascati photo-neutron source. *Nucl. Instr. Meth. A* 659, 373–377.
- Bedogni, R., Esposito, A., Gentile, A., Angelone, M., Pillon, M., 2011a. Comparing active and passive Bonner sphere spectrometers in the 2.5 MeV quasi mono-energetic neutron field of the ENEA Frascati neutron Generator (FNG). *Radiat. Meas.* 46 (12), 1757–1760.
- Domingo, C., Garcia-Fusté, M.J., Morales, E., Amgarou, K., Castelo, J., Sanchez-Doblado, F., 2009. Evaluation of neutron dose received at different organs in radiotherapy treatments using the UAB PADC based dosimeter in an anthropomorphic phantom. *Radiat. Meas.* 44 (9–10), 1073–1076.
- Domingo, C., de-San-Pedro, M., García-Fusté, M.J., Romero, M.T., Amgarou, K., in this issue. Estimation of the response function of a PADC based neutron dosimeter in terms of fluence, Hp(10) and H*.
- Followill, D.S., Nusslin, F., Orton, C.G., 2007. IMRT should not be administered at photon energies greater than 10 MV. *Med. Phys.* 34, 1877–1879.
- Garcia, M.J., Amgarou, K., Domingo, C., Fernandez, F., 2005. Neutron response study of two CR-39 personal dosimeters with air and nylon converters. *Radiat. Meas.* 40 (2–6), 607–611.
- Hall, E.J., Wu, C.S., 2003. Radiation-induced second cancer: the impact of 3D-CRT and IMRT. *Int. J. Radiat. Oncol. Biol. Phys.* 56, 83–88.
- Hall, E.J., Phil, D., 2006. Intensity-modulated radiation therapy, protons, and the risk of second cancers. *Int. J. Radiat. Oncol. Biol. Phys.* 65, 1–7.
- ISO, International Standardization Organization, 2008a. Reference Radiation Fields – Simulated Workplace Neutron Fields – Part 1: Characteristics and Methods of Production. International Standard ISO 12789-1:2008.
- ISO, International Standardization Organization, 2008b. Reference Radiation Fields – Simulated Workplace Neutron Fields – Part 2: Calibration Fundamental Related to the Basic Quantities. International Standard ISO 12789-2:2008.
- Kluge, H., Alevra, A.V., Jetzke, S., Knauf, K., Matzke, M., Weise, K., Wittstock, J., 1996. Scattered neutron reference fields produced by radionuclide sources. *Radiat. Prot. Dosimetry* 70 (1–4), 327–330.
- Thomas, D.J., Bardell, A.G., Macaulay, E.M., 2002. Characterisation of a gold foil-based Bonner sphere set and measurements of neutron spectra at a medical accelerator. *Nucl. Instr. Meth. A* 476, 31–35.
- Waters, L.S. (Ed.), 2002. MCNPXTM Users Manual. ECI, Version 2.4.0, Los Alamos National Laboratory report LA-CP-02-408.